PAPER • OPEN ACCESS

Higher-Twist Mechanism and Inclusive Gluon Production in Pion-Proton Collisions

To cite this article: A. I. Ahmadov *et al* 2016 *J. Phys.: Conf. Ser.* **670** 012001

View the article online for updates and enhancements.

Higher-Twist Mechanism and Inclusive Gluon Production in Pion-Proton Collisions

A. I. Ahmadov[1,2], C. Aydin[3], R. Myrzakulov[4], O. Uzun[3]

[1] Fachbereich C, Bergische Universität Wuppertal, 42097 Wuppertal, Germany,

[2] Department of Theoretical Physics, Baku State University, Z. Khalilov st. 23, AZ-1148, Baku, Azerbaijan,

[3] Department of Physics, Karadeniz Technical University, 61080, Trabzon, Turkey,

[4] Eurasion International Center for Theoretical Physics and Department of General Theoretical Physics, Eurasian National University, Astana 010008, Kazakhstan

E-mail: `ahmadovazar@yahoo.com, coskun@ktu.edu.tr, rmyrzakulov@gmail.com, oguzhan_deu@hotmail.com`

Abstract. We calculate the contribution of the higher-twist Feynman diagrams to the large-p_T inclusive gluon production cross section in πp collisions incase of the running coupling and frozen coupling approaches within perturbative and holographic QCD. The structure of infrared renormalon singularities of the higher-twist subprocess cross section are obtained and the resummed higher-twist cross sections (Borel sum) with the ones obtained in the framework of the frozen coupling approach and leading-twist cross section are compared and analyzed.

1. Introduction

It is well known that Quantum Chromodynamics (QCD) is the fundamental theory of the strong interactions.Therefore in order to describe the structure and dynamical properties of hadrons at the amplitude level many researchers have been studying QCD. The hadronic distribution amplitude in terms of internal structure degrees of freedoms plays a crucial role in QCD process predictions.

One of the basic problems in QCD is choosing the renormalization scale in running coupling constant $\alpha_s(Q^2)$. In principle, in perturbative QCD (pQCD) calculations, the argument of the running coupling constant in both the renormalization and factorization scale Q^2 should be taken as equal to the square of the momentum transfer of a hard gluon in a corresponding Feynman diagram [1]. In the perturbative QCD, the physical information of the inclusive gluon production is obtained efficiently; therefore, it can be directly compared to the experimental data.

It should be noted, that problem the existence of the higher-twist contribution is not yet settled. Also necessary to study the difference of the leading-twist results for the frozen and running coupling constant approaches and compare it with that of the higher-twist is important.

Take into account of this point the aim of this study is calculation and analysis of the inclusive gluon production in the pion-proton collisions using the frozen and running coupling constant approaches. Using this approaches the higher twist effects have been already calculated by many authors [2, 3, 4, 5, 6, 7, 8, 9, 10, 11, 12, 13, 14, 15, 16, 17, 18, 19, 20, 21, 22, 23].

The contents of the paper is as follows. The related formulas for the calculation of the contributions of the higher-twist and leading-twist diagrams are provided in the next section. The formulas and analysis of the higher twist effects on the dependence of the pion distribution amplitudes by the running coupling constant approach are presented in Section 3, and the numerical results for the cross section and discussion of the dependence of the cross section on the pion distribution amplitudes are presented in Section 4. Finally, our conclusions and the highlights of the study are listed in Section 5.

2. HIGHER-TWIST AND LEADING-TWIST CONTRIBUTIONS TO INCLUSIVE GLUON PRODUCTION

The higher-twist Feynman diagrams for the inclusive gluon production in the pion-proton collision $\pi p \to gX$ are shown in Fig.1. For the process $\pi p \to gX$, we write invariant amplitude as in the form (as called by Brodsky-Lepage formula [24])

$$M(\hat{s}, \hat{t}) = \int_0^1 dx_1 \int_0^1 dx_2 \delta(1 - x_1 - x_2)\Phi_M(x_1, x_2, Q^2)T_H(x_1, x_2; Q^2, \mu_R^2, \mu_F^2) \qquad (1)$$

where T_H is the sum of the graphs contributing to the hard-scattering part of the subprocess. For the higher-twist, the subprocess is taken as $\pi q_p \to gq$, which contributes to $\pi p \to gX$, where q_p is a constituent of the initial proton target. As seen from Fig.1, the processes $\pi^+ p \to gX$ and $\pi^- p \to gX$ arise from subprocesses as $\pi^+ d_p \to gu$ and $\pi^- u_p \to gd$, respectively. The production of the hadronic gluon in the large transverse momentum is available at the high energy, especially at the Large Hadron Collider. Finally hadronic gluon is a product of the hard-scattering processes, before hadronization. In the final state, this hadronic gluon is fragmented to hadron. The main dynamical properties of the gluon, which carried one part of the four momentum, are close to the parent parton. In order to understand the parton kinematics one should consider the gluon production process [25]. The higher-twist cross section for $\pi p \to gX$ process has the form:

$$E\frac{d\sigma}{d^3p}(\pi p \to gX) = \int_0^1 dx\delta(\hat{s} + \hat{t} + \hat{u})\hat{s}G_{q/p}(x, Q^2)\frac{1}{\pi}\frac{d\sigma}{d\hat{t}}(\pi q_p \to gq), \qquad (2)$$

where $G_{q/p}(x, Q^2)$ is the quark distribution function inside a proton.

For higher-twist subprocess $\pi q_p \to gq$ the Mandelstam invariant variables are writen in the form:

$$\hat{s} = (p_1 + p_g)^2 = (p_2 + p_\pi)^2, \quad \hat{t} = (p_g - p_\pi)^2, \quad \hat{u} = (p_1 - p_\pi)^2. \qquad (3)$$

Then the parton-level cross section within running coupling constant method becomes

$$\frac{d\sigma}{d\hat{t}}(\pi q_p \to gq) = \frac{256\pi^2}{81\hat{s}^2}[D(\hat{s}, \hat{u})]^2\left(-\frac{\hat{t}}{\hat{s}^2} - \frac{\hat{t}}{\hat{u}^2}\right), \qquad (4)$$

where

$$D(\hat{s}, \hat{u}) = \int_0^1 dx\alpha_s^{3/2}(Q_1^2)\left[\frac{\Phi_\pi(x, Q_1^2)}{x(1-x)}\right] + \int_0^1 dx\alpha_s^{3/2}(Q_2^2)\left[\frac{\Phi_\pi(x, Q_2^2)}{x(1-x)}\right]. \qquad (5)$$

By the way it must be denoted that as a special case we can directly get the result [26] from Eq(4) by the applying the frozen coupling constant approximation.

According BLM approach transfer momentum of the hard gluon in Fig.1 for s and u channels get the forms

$$Q_1^2 = (1 - x)\hat{s} \quad \text{and} \quad Q_2^2 = -x\hat{u}, \qquad (6)$$

respectively.
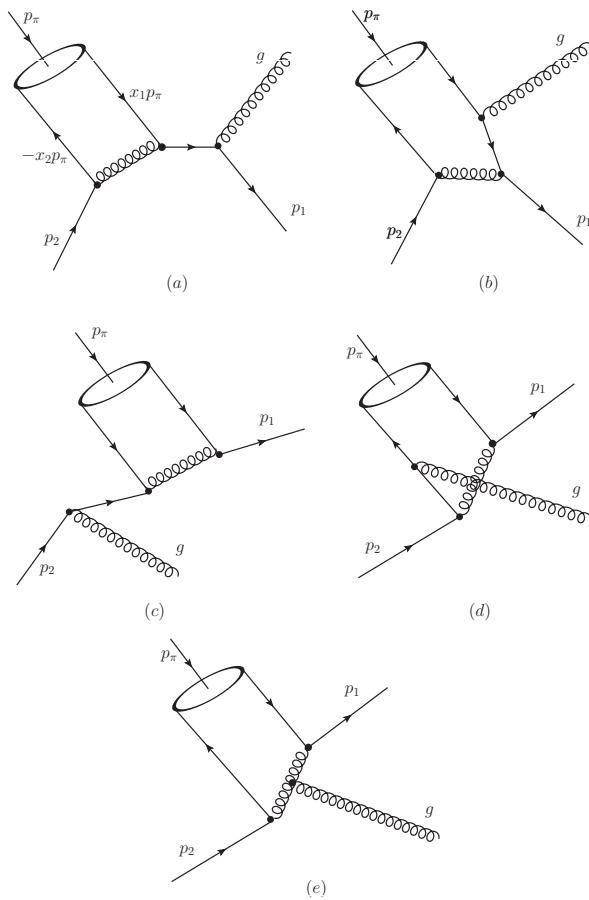
Figure 1. Full set of QCD Feynman diagrams for higher-twist subprocess $\pi q \to gq$.

In the soft regions $x \to 0$ and $x \to 1$ (for u and s channels) integrals (5) diverge, therefore in these regions for their calculations some regularization methods of $\alpha_s(Q^2)$ are needed. One of the simple method is called frozen coupling constant approximation for the regularization these singularity.

There are few forms of the pion distribution amplitude available in the literature. In the present numerical calculations, we use several choices, such as the asymptotic distribution amplitude derived in pQCD evalution [27], the Vega-Schmidt-Branz-Gutsche-Lyubovitskij (VSBGL) distribution amplitude [28], distribution amplitudes predicted by AdS/CFT [30, 29], the Chernyak-Zhitnitsky(CZ) [31], the Bakulev-Mikhailov-Stefanis (BMS) [32] and pion distribution amplitudes in which Gegenbauer coefficients C_2 and C_4 are extracted from BELLE experiment [33, 34]:

$$\Phi_{asy}(x, Q^2 \to \infty) = \sqrt{3} f_\pi x(1-x), \tag{7}$$

$$\Phi_{VSBGL}^{hol}(x, \mu_0^2) = \frac{A_1 k_1}{2\pi} \sqrt{x(1-x)} exp\left(-\frac{m^2}{2k_1^2 x(1-x)}\right), \tag{8}$$

$$\Phi^{hol}(x, \mu_0^2) = \frac{4}{\sqrt{3}\pi} f_\pi \sqrt{x(1-x)}, \tag{9}$$

$$\Phi_{CZ}(x,\mu_0^2) = \Phi_{asy}(x)\left[C_0^{3/2}(2x-1) + \frac{2}{3}C_2^{3/2}(2x-1)\right], \tag{10}$$

$$\Phi_{BMS}(x,\mu_0^2) = \Phi_{asy}(x)\left[C_0^{3/2}(2x-1) + 0.20C_2^{3/2}(2x-1) - 0.14C_4^{3/2}(2x-1)\right], \tag{11}$$

$$\Phi_{BELLE}(x,\mu_0^2) = \Phi_{asy}(x)\left[C_0^{3/2}(2x-1) + 0.12C_2^{3/2}(2x-1) + 0.08C_4^{3/2}(2x-1)\right], \tag{12}$$

here $C_n^\lambda(2x-1)$ are Gegenbauer polynomials.

Substituting Eq.(4) into Eq.(2) then the differential cross section for the process $\pi p \to gX$ takes the form [26]

$$E\frac{d\sigma}{d^3p}(\pi p \to gX) = \frac{s}{s+u}xG_{q/p}(x,Q^2)\frac{256\pi}{81\hat{s}^2}[D(\hat{s},\hat{u})]^2\left(-\frac{\hat{t}}{\hat{s}^2} - \frac{\hat{t}}{\hat{u}^2}\right). \tag{13}$$

It should be noted that, as seen from Eq.(4) and Eq.(13), the higher-twist cross section is linear with respect to $\hat{t}$, so the cross section vanishes, if the scattering angle between the final gluon and incident pion is approximately equal to zero. From Eq.(13) we see that the higher-twist cross section proportional to $\hat{s}^{-3}$, which is equivalent to the higher-twist contributions to the $\pi p \to gX$ cross section have the form of $p_T^{-6}f(x_F,x_T)$.

In the expression (6) we fixed the variable x by taking it is mean value. So, average values for x we take $\overline{x} = 1/2$. Thus, for the calculations higher-twist cross sections within frozen coupling constant approach we substitute $\overline{Q}^2 = \hat{s}/2$ and $\overline{Q}^2 = -\hat{u}/2$ in Eq.(13) for the transfer momentum of the hard gluon, respectively.

The extracting of higher-twist contribution from the inclusive gluon production cross section is also complicated. One can also consider the comparison of higher-twist corrections with leading-twist contributions. For the leading-twist subprocess in the inclusive gluon production, we take $q\bar{q} \to g\gamma$ as a subprocess of the quark-antiquark annihilation. The differential cross section for subprocess $q\bar{q} \to g\gamma$ is

$$\frac{d\sigma}{d\hat{t}}(q\bar{q} \to g\gamma) = \frac{8}{9}\pi\alpha_E\frac{e_q^2}{\hat{s}^2}\left(\alpha_s(-\hat{u})\frac{\hat{t}}{\hat{u}} + \alpha_s(-\hat{t})\frac{\hat{u}}{\hat{t}}\right). \tag{14}$$

As is seen from Eq.(14) leading-twist cross section strongly depend of the running coupling constant where the running coupling constant depends on the transfer momentum. However running coupling constant depends on the channels of the process. Here running coupling have been evaluated in the momentum subtraction scheme, for momentum scales u and t, which define the off-shell momenta carried by the quark propagators.

The leading-twist cross section for production of inclusive gluon is [35]

$$\Sigma_M^{LT} \equiv E\frac{d\sigma}{d^3p}(\pi p \to gX) = \int_0^1 dx_1 \int_0^1 dx_2\delta(\hat{s}+\hat{t}+\hat{u})G_{\bar{q}/M}(x_1,Q_1^2)G_{q/p}(x_2,Q_2^2)\frac{\hat{s}}{\pi}\frac{d\sigma}{d\hat{t}}(q\bar{q} \to g\gamma), \tag{15}$$

where

$$\hat{s} = x_1x_2s, \ \hat{t} = x_1t, \ \hat{u} = x_2u.$$

3. HIGHER TWIST MECHANISM WITHIN PERTURBATIVE AND HOLOGRAPHIC QCD AND THE ROLE INFRARED RENORMALONS

Mainly object of this study is beside the calculations of the higher twist cross section with running coupling constant approach within holographic and perturbative QCD and renormalon effect's contribution to the cross section, and also comparisons between higher-twist cross sections which are calculated by the running coupling constant method and the principle maximum conformality

approach. It should be noted that, in the exclusive processes, the coupling constant α_s runs not only due to the loop integration but also the integration in the process amplitude over the light-cone momentum fraction of hadron constituents. Therefore, it is worth noting that the renormalization scale according to Fig.1 should be chosen equal to $\mu_{R_1}^2 = Q_1^2 = (1-x)\hat{s}$, and $\mu_{R_2}^2 = Q_2^2 = -x\hat{u}$. The integral in Eq.(5) in the framework of the running coupling approach takes the form

$$D(\mu_R^2) = \int_0^1 \frac{\alpha_s^{3/2}((1-x)\hat{s})\Phi_M(x,\mu_F^2)dx}{x(1-x)} + \int_0^1 \frac{\alpha_s^{3/2}(-x\hat{u})\Phi_M(x,\mu_F^2)dx}{x(1-x)}. \tag{16}$$

At the leading order of perturbative QCD calculations the hard scattering amplitude $T_H(x_1,x_2;Q^2,\mu_R^2,\mu_F^2)$ does not depend on the factorization scale μ_F^2, but strongly depends on μ_R^2. The one-loop QCD correction to the hard scattering amplitude $T_H(x_1,x_2;Q^2,\mu_R^2,\mu_F^2)$ generates its explicit dependence on the scales μ_F^2 and μ_R^2.

As we noted above in the regions $x \to 0$ and $x \to 1$ the integral (16) diverges, because in this regions running coupling constants $\alpha_s((1-x)\hat{s})$ and $\alpha_s(-x\hat{u})$ have the infrared singularity. The other words the singularity of the integrand of x=0 and x=1 is due to only by $\alpha_s((1-x)\hat{s})$ and $\alpha_s(-x\hat{u})$. Thus for the regularization of the integral, by expressing the running coupling at scaling variable $\alpha_s(\mu_R^2)$, we use renormalization group equation with the fixed $\alpha_s(\hat{s})$ and $\alpha_s(-\hat{u})$ for s and u channels, respectively. The solution of renormalization group equation for the running coupling $\alpha \equiv \alpha_s/\pi$ is in the form [22]

$$\frac{\alpha(\lambda)}{\alpha} = \left[1 + \alpha\frac{\beta_0}{4}\ln\lambda\right]^{-1}. \tag{17}$$

Then, for $\alpha_s((1-x)\hat{s})$, we get

$$\alpha((1-x)s) = \frac{\alpha_s}{1 + ln(1-x)/t} \tag{18}$$

where $t = 4\pi/\alpha_s(Q^2)\beta_0 = 4/\alpha\beta_0$.

If we insert Eq.(18) into Eq.(16), we obtain

$$D(\hat{s},\hat{u}) = \int_0^1 dx \frac{\alpha_s^{3/2}((1-x)\hat{s})\Phi_\pi(x,Q_1^2)}{x(1-x)} + \int_0^1 dx \frac{\alpha_s^{3/2}(-x\hat{u})\Phi_\pi(x,Q_2^2)}{x(1-x)}$$

$$= \alpha_s^{3/2}(\hat{s})t_1^{3/2}\int_0^1 dx \frac{\Phi_\pi(x,Q_1^2)}{x(1-x)(t_1 + \ln\lambda_1)^{3/2}} + \alpha_s^{3/2}(-\hat{u})t_2^{3/2}\int_0^1 dx \frac{\Phi_\pi(x,Q_2^2)}{x(1-x)(t_2 + \ln\lambda_2)^{3/2}} \tag{19}$$

where $t_1 = 4\pi/\alpha_s(\hat{s})\beta_0$ and $t_2 = 4\pi/\alpha_s(-\hat{u})\beta_0$.

Although the integral (19) is still has singularity, this expression can be transformed to more convenient form by the change of variable as, $z = \ln\lambda$ and after applying the integral representation of $1/(t+z)^\nu$ [36, 37],

$$\frac{1}{(t+z)^\nu} = \frac{1}{\Gamma(\nu)}\int_0^\infty e^{-(t+z)u}u^{\nu-1}du, Re\nu > 0 \tag{20}$$

then the singularity in (19) disappears and we obtain

$$D(\hat{s},\hat{u}) = \frac{\alpha_s^{3/2}(-\hat{s})t_1^{3/2}}{\Gamma(\frac{3}{2})}\int_0^1\int_0^\infty \frac{\Phi_\pi(x,Q_1^2)e^{-(t_1+z_1)u}u^{1/2}dudx}{x(1-x)} +$$

$$+\frac{\alpha_s^{3/2}(-\hat{u})t_2^{3/2}}{\Gamma(\frac{3}{2})}\int_0^1\int_0^\infty \frac{\Phi_\pi(x,Q_2^2)e^{-(t_2+z_2)u}u^{1/2}dudx}{x(1-x)}, \tag{21}$$
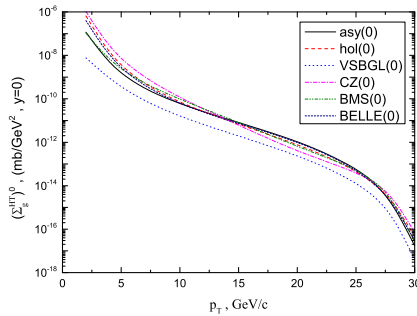
Figure 2. Higher-twist $\pi^+ p \rightarrow gX$ inclusive gluon production cross section $(\Sigma_g^{HT})^0$ as a function of the transverse momentum of the gluon p_T at the c.m. energy $\sqrt{s} = 62.4\ GeV$.
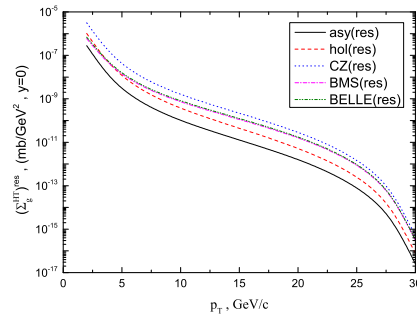
Figure 3. Higher-twist $\pi^+ p \rightarrow gX$ inclusive gluon production cross section $(\Sigma_g^{HT})^{res}$ as a function of the transverse momentum of the gluon p_T at the c.m.energy $\sqrt{s} = 62.4\ GeV$.

Then the Eq.(21) can be written, for $\Phi^{hol}(x, Q^2)$, as

$$D(\hat{s}, \hat{u}) = \frac{32\sqrt{\pi} f_\pi}{\beta_0 \sqrt{3\beta_0} \Gamma(\frac{3}{2})} \int_0^\infty du e^{-t_1 u} u^{1/2} B\left(\frac{1}{2}, \frac{1}{2} - u\right) + \frac{32\sqrt{\pi} f_\pi}{\beta_0 \sqrt{3\beta_0} \Gamma(\frac{3}{2})} \int_0^\infty du e^{-t_2 u} u^{1/2} B\left(\frac{1}{2}, \frac{1}{2} - u\right),$$

$$(22)$$

for $\Phi_{asy}(x, Q^2 \rightarrow \infty)$ distribution amplitude, as

$$D(\hat{s}, \hat{u}) = \frac{8\pi\sqrt{3\pi} f_\pi}{\beta_0 \sqrt{\beta_0} \Gamma(\frac{3}{2})} \int_0^\infty du e^{-t_1 u} \left[\frac{u^{1/2}}{1-u}\right] + \frac{8\pi\sqrt{3\pi} f_\pi}{\beta_0 \sqrt{\beta_0} \Gamma(\frac{3}{2})} \int_0^\infty du e^{-t_2 u} \left[\frac{u^{1/2}}{1-u}\right], \quad (23)$$

for $\Phi_{CZ}(x, Q^2)$ distribution amplitude, as

$$D(\hat{s}, \hat{u}) = \frac{8\pi\sqrt{3\pi} f_\pi}{\beta_0 \sqrt{\beta_0} \Gamma(\frac{3}{2})} \int_0^\infty du e^{-t_1 u} u^{1/2} \left[\frac{1}{1-u} + 0.84\left[\frac{4}{1-u} - \frac{20}{2-u} + \frac{20}{3-u}\right] \left(\frac{\alpha_s(Q_1^2)}{\alpha_s(\mu_0^2)}\right)^{\frac{50}{81}}\right] +$$

$$\frac{8\pi\sqrt{3\pi} f_\pi}{\beta_0 \sqrt{\beta_0} \Gamma(\frac{3}{2})} \int_0^\infty du e^{-t_2 u} u^{1/2} \left[\frac{1}{1-u} + 0.84\left[\frac{4}{1-u} - \frac{20}{2-u} + \frac{20}{3-u}\right] \left(\frac{\alpha_s(Q_2^2)}{\alpha_s(\mu_0^2)}\right)^{\frac{50}{81}}\right].$$

$$(24)$$

4. NUMERICAL RESULTS AND DISCUSSION

We discuss the numerical results for higher-twist and renormalon mechanism with higher-twist contributions calculated in the context of the running and frozen coupling approaches on the dependence of the chosen pion distributions amplitudes in the inclusive gluon production process. For the numerical calculations, we take supprocess $\pi^+ d_p \rightarrow gu$ and $\pi^- u_p \rightarrow gd$ for $\pi^+ p \rightarrow gX$ and $\pi^- p \rightarrow gX$ process, respectively.

Inclusive direct gluon production represents a significant test case in which higher-twist terms dominate those of leading-twist in certain kinematic domains. For the dominant leading-twist subprocess for the gluon production, we take the quark-antiquark annihilation $q\bar{q} \rightarrow \gamma g$. In the numerical calculations, for the quark distribution functions inside the pion and proton we used expressions as given in [38, 39], respectively. Results obtained in our calculations are visualized in Figs. 2-7. In all figures we represent the choice of pion distribution amplitudes
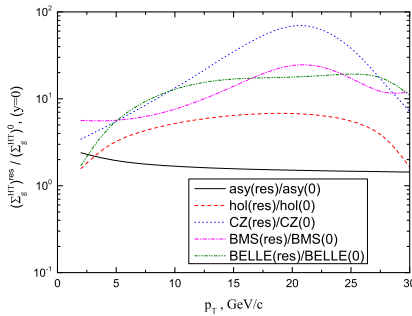
Figure 4. Ratios $(\Sigma_g^{HT})^{res}/(\Sigma_g^{HT})^0$, in the process $\pi^+ p \to gX$, where higher-twist contribution are calculated for the gluon rapidity $y = 0$ at the c.m.energy $\sqrt{s} = 62.4\ GeV$ as function of the gluon transverse momentum, p_T.
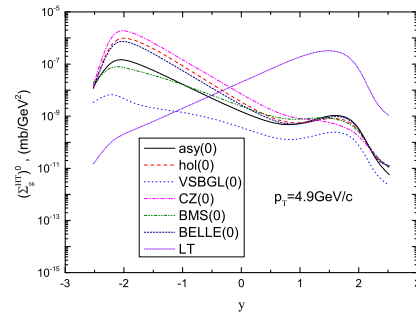
Figure 5. Higher-twist $\pi^+ p \to gX$ inclusive gluon production cross section $(\Sigma_g^{HT})^0$, as function of the rapidity of the gluon y at the transverse momentum of the gluon $p_T = 4.9\ GeV/c$, at the c.m. energy $\sqrt{s} = 62.4\ GeV$.

Eqs.(7)-(12) by different line types: $\Phi_{asy}(x)$ as solid black line, $\Phi^{hol}(x)$ as dashed red line, $\Phi_{VSBGL}^{hol}(x)$ as dotted blue line, $\Phi_{CZ}(x, Q^2)$ as dash-dot magenta line, $\Phi_{BMS}(x, Q^2)$ as dash-double dot olive line, and $\Phi_{BELLE}(x, Q^2)$ as short dash navy line. Firstly, it is very interesting to compare the higher-twist cross sections obtained within holographic QCD with ones obtained within the perturbative QCD and also with the leading-twist cross section. In Fig.2 and Fig.3 we show higher-twist cross sections $(\Sigma_g^{HT})^0$, $(\Sigma_g^{HT})^{res}$ calculated in the context of the frozen (frozen cross section) and running coupling constant (resummed cross section) approaches as a function of the gluon transverse momentum p_T for the pion distribution amplitudes presented in Eqs.(2.6)-(2.11) at $y = 0$. It is seen from Fig.2 and Fig.3 that the higher-twist cross section is monotonically decreasing with an increase in the transverse momentum of the gluon. In the region $2\ GeV/c < p_T < 30\ GeV/c$ the resummed cross sections of the process $\pi^+ p \to gX$ decreases in the range between $3,172 \cdot 10^{-6} \mu b/GeV^2$ to $4,912 \cdot 10^{-16} \mu b/GeV^2$.

In Fig.4 we show $(\Sigma_g^{HT})^{res}/(\Sigma_g^{HT})^0$, for the process $\pi^+ p \to gX$ as a function of p_T for the pion distribution amplitudes presented in Eqs.(7)-(12) at $y = 0$. We see in Fig.4, that in the region $15\ GeV/c < p_T < 22\ GeV/c$, the ratio $(\Sigma_g^{HT})^{res}/(\Sigma_g^{HT})^0$ for $\Phi_{CZ}(x, Q^2)$ is enhanced by about two orders of magnitude relative to one for $\Phi_{asy}(x)$. However, the enhancement is one order of magnitude for $\Phi^{hol}(x)$ and half an order for $\Phi_{BMS}(x, Q^2)$ and $\Phi_{BELLE}(x, Q^2)$ pion distribution amplitudes. Through Fig.5 to Fig.7 the dependence of higher-twist cross sections $(\Sigma_g^{HT})^0$, $(\Sigma_g^{HT})^{res}$, ratios $(\Sigma_g^{HT})^{res}/(\Sigma_g^{HT})^0$ are shown for the processes $\pi^+ p \to \gamma X$ and $\pi^- p \to \gamma X$ as a function of the rapidity of the gluon y at the transverse momentum of the gluon $p_T = 4.9\ GeV/c$. It is seen from figures in Fig.5 and Fig.6, that frozen and resummed cross sections for all distribution amplitudes of pion have two maxima, where the first maximum is approximately at the point $y = -2$ and second maximum is approximately at the point $y = 2$. Notice that distribution amplitude of frozen and resummed cross sections for $\Phi_{CZ}(x, Q^2)$ are enhanced by about half and two orders of magnitude relative to all other distribution amplitudes. As is seen from the figures cross sections vary slowly and smoothly with the angle of the scattering. We think that this feature of infrared renormalons may help theoretical interpretations of the future experimental data for the direct inclusive gluon production cross section in the pion-proton collisions. Higher-twist cross section obtained in our study should be observable at hadron collider.
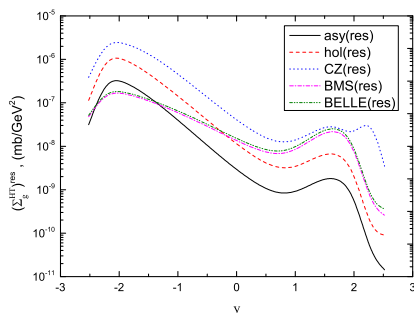
Figure 6. Higher-twist $\pi^+ p \to gX$ inclusive gluon production cross section $(\Sigma_g^{HT})^{res}$, as a function of the rapidity of the gluon y at the transverse momentum of the gluon $p_T = 4.9 \ GeV/c$, at the c.m. energy $\sqrt{s} = 62.4 \ GeV$.
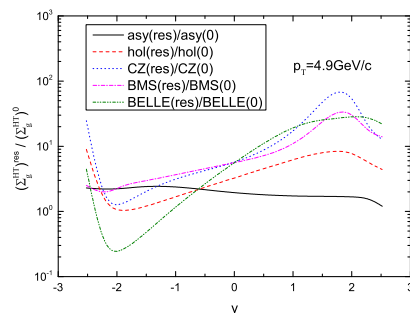
Figure 7. Ratio $(\Sigma_g^{HT})^{res}/(\Sigma_g^{HT})^0$, in the process $\pi^+ p \to gX$, as function of the rapidity of the gluon y at the transverse momentum of the gluon $p_T = 4.9 \ GeV/c$, at the c.m. energy $\sqrt{s} = 62.4 \ GeV$.

5. CONCLUSIONS

In this study the inclusive single gluon production are calculated via higher twist mechanism within perturbative and holographic QCD. In the calculation of the cross sections the running and frozen coupling constant approaches are employed and infrared renormalon poles in the cross section expression are revealed. Infrared renormalon induced divergences are regularized by means of the principal value prescripton and the Borel sum for the higher twist cross section is found. It is observed that, the resummed higher-twist cross section differs from that found using the frozen coupling approximation, especially in some regions, considerably.

Concerning the study of the higher-twist contribution, it is primarily important to analyze its relative magnitude of contribution compared to the leading-twist contribution, since only leading-twist diagrams are commonly considered in usual studies of the hadron-hadron collision. However, in our studies the difference of the higher-twist results for the frozen and running coupling constant approaches have been studied with importance. The following results can be concluded from the experiments: the higher-twist contributions to single gluon production cross section in the pion-proton collisions have important phenomenological consequences. Therefore they will be helpful for detailed investigation dynamical properties of nucleon. Also the higher-twist gluon production cross section in the pion-proton collisions depends on the form of the pion distribution amplitudes and may be used for future study. Moreover the contributions of renormalon effects within holograpich QCD in these process are essential and may help to analyze experimental results. We compared frozen and resumed cross sections of the direct gluon production in the processes $\pi^- p \to gX$ and $\pi^+ p \to gX$. Our calculations show in both cases, running and frozen coupling constant approaches that the inclusive gluon production cross section for the process $\pi^- p \to gX$ is suppress over the direct gluon production cross section of the process $\pi^+ p \to gX$. Notice that, the direct gluon production spectrum can be measured with large precision, so results obtained in this study will helpful further tests of the hadron dynamics at large p_T. As is seen from Eqs.(4,13) higher- twist cross sections in both cases are proportional to the third power of $\alpha_s(Q^2)$, but the leading-twist is linearly proportional to $\alpha_s(Q^2)$. Therefore their ratios strongly depend on the $\alpha_s^2(Q^2)$.

Further investigations are needed in order to clarify the role of higher-twist effects in QCD. In hadron-hadron collisions, real gluons at high transverse momentum can serve as a short distance probe of the incident hadrons. Especially, the future experimental measurements will provide

further tests of the dynamics of large-p_T hadron production beyond the leading twist.

Acknowledgments

[1] S. J. Brodsky, G. L. Lepage, and P. B. Mackenize, Phys. Rev. D **28** (1983) 228.
[2] F. S. Sadykhov and A. I. Akhmedov, Russ. Phys. J. **38** (1995) 513.
[3] A. I. Ahmadov, I. Boztosun, R. Kh. Muradov, A. Soylu, and E. A. Dadashov, Int. J. Mod. Phys. E **15** (2006), 1209.
[4] A. I. Ahmadov, I. Boztosun, A. Soylu, and E. A. Dadashov, Int. J. Mod. Phys. E **17** (2008), 1041.
[5] A. I. Ahmadov, C. Aydin, Sh. M. Nagiyev, A. Hakan Yilmaz, and E. A. Dadashov, Phys. Rev. D **80** 016003 (2009) 016003.
[6] A. I. Ahmadov, C. Aydin, E. A. Dadashov, and Sh. M. Nagiyev, Phys. Rev. D **81** (2010) 054016.
[7] A. I. Ahmadov, R. M. Burjaliyev, Int. J. Mod. Phys. E **20** (2011) 1243.
[8] A. I. Ahmadov, Sh. M. Nagiyev, and E. A. Dadashov , Int. J. Mod. Phys. E **21** (2012) 1250014.
[9] A. I. Ahmadov, C. Aydin, and F. Keskin, Phys. Rev. D **85** (2012) 034009.
[10] A. I. Ahmadov, C. Aydin, and F. Keskin, Ann. Phys. **327** (2012) 1472.
[11] A. I. Ahmadov, C. Aydin, and O. Uzun, Phys. Rev. D **87** (2013) 014006.
[12] A. I. Ahmadov, C. Aydin, and O. Uzun, Phys. Rev. D **89** (2014) 014018.
[13] J. A. Bagger and J. F. Gunion, Phys. Rev. D **29** (1984) 40.
[14] A. Bagger and J. F. Gunion, Phys. Rev. D **25** (1982) 2287.
[15] V. N. Baier and A. Grozin, Phys. Lett.B **96** (1980) 181; S. Gupta, Phys. Rev. D**24** (1981) 1169.
[16] S. S. Agaev, Phys. Lett.B **360** (1995) 117; **369**, (1996) 379(E).
[17] G.'t. Hooft, in The Whys of Subnuclear Physics, Erice, 1977, edited by A. Zichichi (Plenum, New York, 1979) p.94
[18] A. H. Mueller, Nucl. Phys.B **250** (1985)327; Phys. Lett. **B 308** (1993) 355.
[19] V. I. Zakharov, Nucl. Phys.B **385** (1992) 452.
[20] M. Beneke, Phys. Rep. **317** (1999) 1.
[21] W. Greiner, S. Schramm and E. Stein, Quantum Chromodynamics, 3rd edn.(Berlin, Springer, 2007), pp.553.
[22] H. Contopanagos and G. Sterman, Nucl. Phys.B **419** (1994) 77.
[23] A. L. Kataev, JETP Lett. **81** (2005) 608; Mod. Phys. Lett. **A 20** (2005) 2007.
[24] G. L. Lepage and S. J. Brodsky, Phys. Rev. D **22** (1980) 2157.
[25] J.F. Owens, Rev. Modern Phys. **59** (1987) 465.
[26] E. L. Berger and S. J. Brodsky, Phys. Rev. D **24** (1981) 2428.
[27] G. P. Lepage and S. J. Brodsky, Phys. Lett.B **87** (1979) 359.
[28] A. Vega, I. Schmidt, T. Branz, T.Gutsche, V. Lyubovitskij, Phys. Rev. D **80** (2009) 055014.
[29] S. J. Brodsky and G. F. de Teramond, Phys. Rev. D **77** (2008) 056007.
[30] S. J. Brodsky, Proc. Sci., LHC07 (2007) 002.
[31] V. L. Chernyak and A. R. Zhitnitsky, Phys. Rep. **112** (1984) 173.
[32] A. P. Bakulev, S. V. Mikhailov and N. G. Stefanis, Phys. Lett, **B 578** (2004) 91; A. P. Bakulev, S.V. Mikhailov, A.V. Pimikov, and N. G. Stefanis, Phys. Rev. D **86** (2012) 031501.
[33] S. S. Agaev, V. M. Braun, N. Offer. F. A. Porkort, Phys. Rev. D**86** (2012) 077504.
[34] S. Uehara et al. [Belle Collaboration], Phys. Rev. D **86** 092007 (2012) 092007.
[35] E. L. Berger, Phys. Rev. D **26** (1982) 105.
[36] J. Zinn-Justin, Phys. Rept. **70** (1981) 109.
[37] A. Erdelyi, Higher Transcendental Functions (McGrow-Hill Book Company, New York, 1953), Vol.2.
[38] S.-i Nam, Phys. Rev. D **86** (2012) 074005.
[39] A.D. Martin, W. J. Stirling, R.S. Thorne, G. Watt, Eur. Phys. J. C **63** (2009) 189.